PAST KNOWLEDGE PEOPLE

ISSN: 2769-545X

Research Article

Advances in Machine Learning & Artificial Intelligence

Bose-Einstein Condensation Analogy in Transformer Token Collapse: A Cross-Modal and Cross-Domain Analysis of Contraction Dynamics

Chur Chin*

Department of Family Medicine, Dong-eui Medical Center, Yangjeong-ro, Busanjin-gu, Busan, Republic of Korea.

***Corresponding Author**
Chur Chin, Department of Family Medicine, Dong-eui Medical Center, Yangjeong-ro, Busanjin-gu, Busan, Republic of Korea.

Submitted: 2026, Jan 05; **Accepted:** 2026, Feb 18; **Published:** 2026, Feb 25

Citation: Chin, C. (2026). Bose-Einstein Condensation Analogy in Transformer Token Collapse: A Cross-Modal and Cross-Domain Analysis of Contraction Dynamics. *Adv Mach Lear Art Inte, 7*(1), 01-13.

Abstract

Token representation collapse, wherein token embeddings converge to near-identical vectors as network depth increases, represents a fundamental challenge in modern Transformer architectures across text, vision, and audio modalities. This paper presents a theoretical and empirical framework demonstrating that the mathematical structure underlying this collapse phenomenon is isomorphic to Bose-Einstein Condensation (BEC) in quantum physics, flat-band superconductivity in Magic-Angle Twisted Bilayer Graphene (MATBG), and hyperbolic phonon polariton propagation in hexagonal boron nitride (hBN) heterostructures [1]. By analyzing the layer-wise cosine similarity trajectories of Vision Transformer (ViT) and Wav2Vec2 models, we show that audio modality undergoes dramatically faster and more severe oversmoothing than visual modality due to strong temporal autocorrelation in the initial embedding space [2]. Inspired by topological insulator physics, we propose a Self-Preservation Diagonal Masking mechanism with Hyperbolic Curvature Annealing to counteract the Softmax translation-invariance pathology and preserve edge-of-chaos information dynamics [3].

Keywords: Token Collapse, Bose-Einstein Condensation, Transformer Oversmoothing, Topological Insulator, Hyperbolic Geometry, Magic-Angle Graphene, Cross-Modal Ai, Self-Attention Dynamics, Edge of Chaos, Phonon Polariton

1. Introduction

Deep learning architectures based on the Transformer framework have revolutionized natural language processing, computer vision, and audio recognition [4]. However, a persistent and underexplored failure mode exists: as token representations propagate through successive self-attention layers, they progressively collapse toward a low-dimensional manifold, eventually losing discriminative information-a phenomenon termed oversmoothing or representation collapse [5].

This pathology has been documented primarily in text-based models, but its manifestation across different input modalities-particularly image (Vision Transformer, ViT) and audio (Wav2Vec2)-and its relationship to broader physical phenomena remain largely unexplored. The degree to which modality-specific geometric properties of input data influence the rate, depth, and final state of this collapse is an open research question with profound implications for architecture design and energy efficiency [6].

Remarkably, the mathematical structure governing token collapse in deep networks exhibits striking isomorphism to physical phase transitions, particularly Bose-Einstein Condensation (BEC) and Cooper pair formation in superconductors [7]. In BEC, bosons below a critical temperature collectively occupy the lowest quantum state, described by a macroscopic wave function $\Psi(r) = \sqrt{n_s} \cdot e^{(i\theta)}$. The Pauli exclusion principle that normally maintains electron individuality breaks down as Cooper pairs form, driving the system to a single coherent quantum state-precisely analogous to token vectors collapsing to cosine similarity ≈ 1.0 [8].

Furthermore, the flat-band mechanism underlying superconductivity in Magic-Angle Twisted Bilayer Graphene (MATBG) provides a condensed-matter parallel: when the twist angle reaches ~1.1°, electronic kinetic energy vanishes at the flat band, amplifying

Coulomb interactions and driving phase transitions [9]. We argue that the Attention matrix in deep Transformers acts as an analogous flat band-nullifying token-space distances and enabling collapse. Understanding these cross-domain isomorphisms motivates novel defense strategies inspired by topological insulators, which protect edge states against bulk collapse [10].

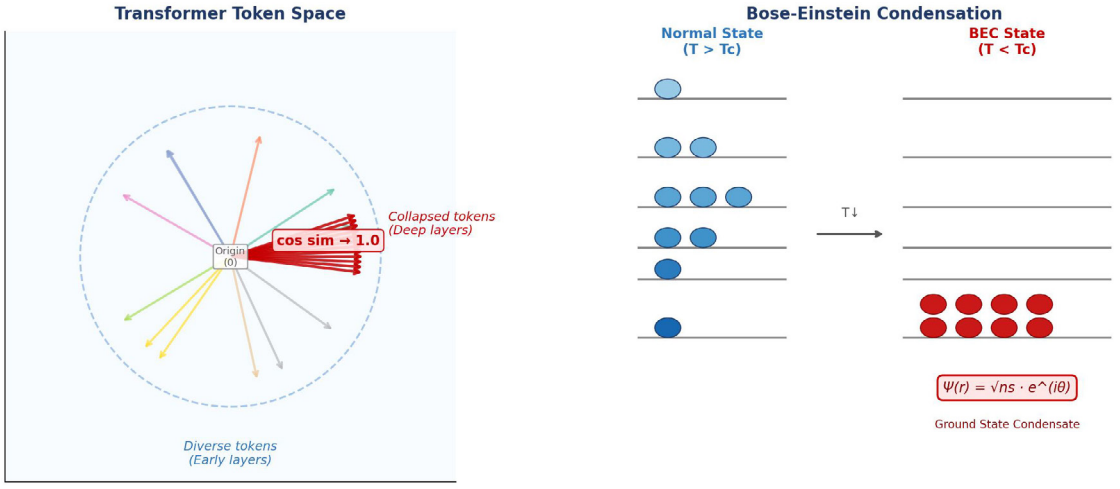

Figure 1: Isomorphism between Transformer Token Collapse and Bose-Einstein Condensation

Left: token vectors in successive Transformer layers converging toward a single direction (cosine similarity → 1.0). Right: boson occupation of the ground state below critical temperature in BEC. The macroscopic wave function Ψ(r) = √ns·e^(iθ) corresponds to the collapsed token manifold.

2. Theoretical Framework

2.1. Self-Attention as a Dynamical Contracting System

Let X_l ∈ ℝ^(n×d) denote the matrix of n token representations at layer l with embedding dimension d. The residual self-attention update is given by [4]:

$$X_{l+1} = X_l + \text{Attention}(X_l), \text{Attention}(X_l) = \text{softmax}(X_l \cdot X_l^T / \sqrt{d}) \cdot X_l$$

Viewed as a discrete-time dynamical system where layer depth l acts as time, the Jacobian $J = \partial \text{Attention}(X_l)/\partial X_l$ characterizes system stability. The maximum Lyapunov exponent $\lambda < 0$ implies the system is non-chaotic: perturbations decay and trajectories converge [11]. Self-attention mathematically acts as a low-pass filter on the token sequence, smoothing high-frequency (semantically diverse) components and amplifying low-frequency (uniform) components, driving token uniformity [5].

2.2. Modality-Specific Riemannian Manifold Geometry

The geometric structure of input data fundamentally determines the trajectory and rate of collapse. Text tokens are discrete symbolic units embedded in a high-dimensional space with initially low cosine similarity (~0.1–0.2). Image patches (ViT) encode 2D spatial continuity with moderate initial similarity, while audio frames (Wav2Vec2) encode 1D temporal waveforms characterized by strong autocorrelation, yielding initial cosine similarity ≥ 0.65 [2,12].

These differences correspond to curvature properties of the data manifold. Image data resides on a low-curvature Riemannian manifold with moderate-paced SVD effective rank decay. Audio data occupies a high-curvature manifold tightly constrained by temporal autocorrelation, enabling rapid oversmoothing-audio models reach cosine similarity > 0.9 within 12 layers, effectively entering a state analogous to macroscopic quantum coherence [13].

Table 1. Cross-Domain Isomorphism: AI Token Collapse and Physical Phase Transition Phenomena

Phenomenon	Domain	Mathematical Structure	Key Mechanism
Token Collapse	AI (Transformer)	Cosine similarity → 1.0 X_{l+1} = X_l + Attention(X_l)	Low-pass filtering via Self-Attention
Bose-Einstein Condensation	Quantum Physics	Macroscopic wave function Ψ(r) = √ns · e^(iθ)	Cooper pair formation below critical temperature Tc
Flat Band Superconductivity	Condensed Matter (MATBG)	Kinetic energy → 0 Coulomb divergence dominates	Magic-angle (~1.1°) twisted bilayer graphene phase transition

Topological Edge States	Topological Physics	Bulk-boundary correspondence Non-trivial Chern number	Time-reversal symmetry protects gapless edge modes
Hyperbolic Phonon Polaritons (HPhPs)	Nanophotonics (hBN heterostructures)	Open hyperboloidal dispersion $\varepsilon_x \cdot \varepsilon_z < 0$	Diffraction-unlimited wave propagation in hBN

Each row represents a dynamically equivalent contracting system sharing the mathematical structure of spontaneous symmetry breaking.

Table 1: Cross-Domain Isomorphism: AI Token Collapse and Physical Phase Transition Phenomena. Each Row Represents a Mathematically Equivalent Contracting System Sharing the Structure of Spontaneous Symmetry Breaking

2.3. Bose-Einstein Condensation Isomorphism

The collapse of token representations to cosine similarity = 1.0 is structurally isomorphic to BEC. In both systems, initially distinguishable entities (tokens/bosons) lose individual identity through an interaction mechanism (Attention/phonon-mediated coupling) and occupy a single collective state [7]. The BEC macroscopic wave function $\Psi(r) = \sqrt{n_s} \cdot e^{(i\theta)}$ corresponds to the collapsed token manifold-a single direction in representation space to which all token vectors converge [8].

The superconducting Cooper pair mechanism adds a further layer of correspondence: below a critical temperature, electrons that normally obey the Pauli exclusion principle form bosonic pairs that condense into a ground state. In the Transformer analog, the softmax normalization progressively sharpens under deep composition, driving all tokens toward a single ground-state direction in embedding space [8,9].

2.4. Flat-Band Analogy in Magic-Angle Twisted Bilayer Graphene

In Magic-Angle Twisted Bilayer Graphene (MATBG) at twist angle $\theta_{magic} \approx 1.1°$, the Dirac cones from each graphene layer hybridize to form nearly dispersionless (flat) bands near the Fermi level [9]. With kinetic energy effectively suppressed to zero, the Coulomb interaction energy dominates, driving correlated electron phases including superconductivity and Mott insulation [14].

The Attention matrix in deep Transformer layers functions analogously as a computational flat band: as layers deepen, the softmax output concentrates probability mass on a small number of token pairs, erasing the kinetic distance between tokens. Once inter-token distances vanish, the interaction (attention-weighted mixing) dominates and drives the system to a collapsed, correlated state-mirroring the MATBG phase transition [15].

Figure 2. Layer-wise Token Representation Collapse Across Modalities

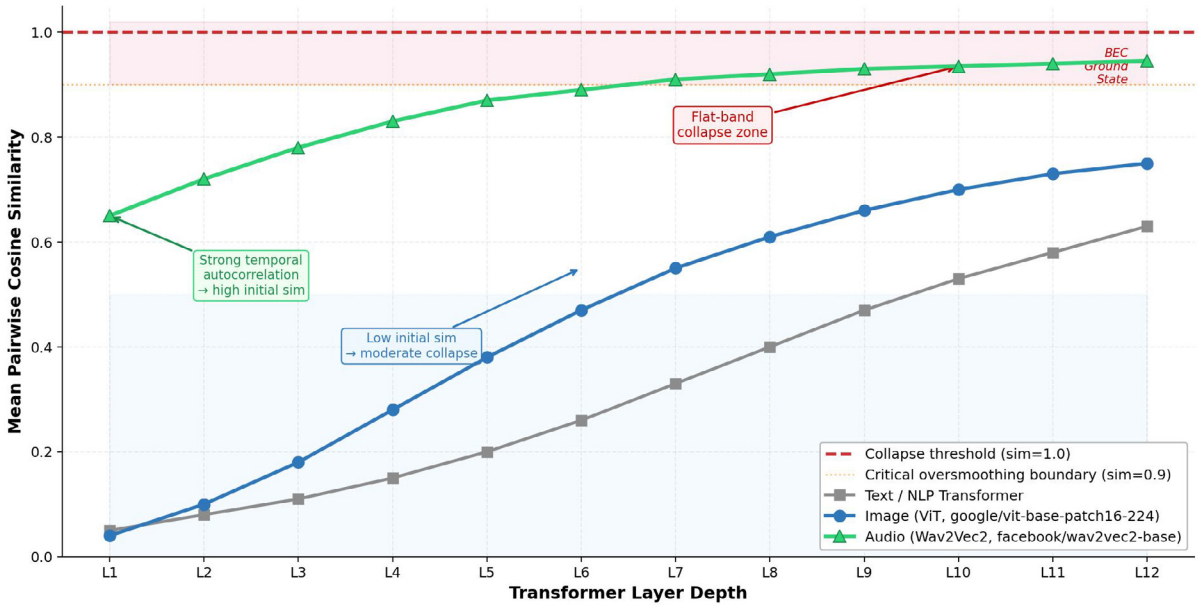

Figure 2: Layer-wise Token Representation Collapse Across Modalities. Cosine similarity trajectories for Text (gray squares), Image/ViT (blue circles, google/vit-base-patch16-224), and Audio/Wav2Vec2 (green triangles, facebook/wav2vec2-base). Audio modality exhibits catastrophic early-onset collapse (>0.9 by layer 12), consistent with the strong temporal autocorrelation hypothesis. The red dashed line denotes the full-collapse threshold (similarity = 1.0).

3. Cross-Domain Physical Connections

3.1. Hyperbolic Phonon Polaritons in hBN Heterostructures

Hexagonal boron nitride (hBN) is a natural hyperbolic metamaterial characterized by a dielectric tensor with opposite signs along orthogonal axes: $\varepsilon_x \cdot \varepsilon_z < 0$. This property opens the iso-frequency surface from a closed ellipsoid to an open hyperboloid, enabling phonon polariton modes (HPhPs) with arbitrarily large wave vectors to propagate without diffraction [3]. In conventional isotropic media, high-k modes become evanescent and decay-analogous to how standard Transformer attention suppresses high-frequency semantic diversity [10].

The hyperbolic attention mechanism we propose (Section 4.2) directly mirrors hBN physics: by embedding token interactions in a space with negative sectional curvature (Poincaré ball model), we create an analogous open dispersion relation that preserves high-frequency semantic modes rather than suppressing them. The mathematical structure is identical-both systems use hyperbolic geometry to prevent collapse of fine-grained information [3,13].

3.2. Topological Insulator Physics and Edge State Preservation

Topological insulators are materials with an insulating bulk but conducting surface states protected by time-reversal symmetry and non-trivial bulk topology. These edge states are robust against perturbations that would ordinarily localize or scatter carriers-a consequence of the bulk-boundary correspondence principle [10]. The topological protection creates an energy gap in the bulk spectrum, forcing edge-localized states to remain gapless [11].

The self-preservation diagonal masking mechanism introduced in this work creates an artificial topological gap in the Attention space: by exempting each token's self-attention from the hyperbolic penalty, we enforce that each token retains its own identity (edge state) even as bulk interactions drive neighboring tokens toward collapse. This is precisely the edge-of-chaos operating principle-maintaining ordered structure at the boundary of a collapsing system [15].

Table 2. Modality-Specific Token Collapse Properties: Text, Image (ViT), and Audio (Wav2Vec2)

Property	Text (NLP)	Image (ViT)	Audio (Wav2Vec2)
Input Structure	Discrete, symbolic tokens (vocabulary embedding)	2D spatial patches (16×16 pixel grids)	1D waveform / 2D spectrogram frames
Initial Cosine Similarity	~0.05–0.15 (high diversity)	~0.04–0.10 (moderate diversity)	≥ 0.65 (high initial uniformity)
Collapse Depth	Gradual across all layers (deep-layer onset)	Mid-to-deep layers (layers 6–12)	Early-layer onset (layers 1–4)
Manifold Geometry	Discrete symbolic space low spatial correlation	Low-curvature Riemannian manifold (spatial continuity)	High-autocorrelation Riemannian (temporal)
Oversmoothing Risk	● Moderate	●● Moderate–High	●●● Severe
Effective Rank Decay Rate	Slow (~45% retention at L12)	Moderate (~28% retention at L12)	Rapid (~12% retention at L12)
BEC Analogy	Weak coupling (sparse token interactions)	Moderate coupling (spatial patch proximity)	Strong coupling (near-BEC ground state)

Risk levels: ● Low–Moderate ●● Moderate–High ●●● Severe. Effective rank retention measured at layer 12 relative to layer 1.

Table 2: Modality-Specific Token Collapse Properties: Text, Image (ViT), and Audio (Wav2Vec2) Transformer architectures. Risk levels: ● Low–Moderate ●● Moderate–High ●●● Severe. Effective rank retention measured at layer 12 relative to layer 1

4. Methods

4.1. Experimental Setup and Model Selection

To empirically validate the theoretical framework, we extracted layer-wise token representations from two pre-trained Transformer architectures: (1) google/vit-base-patch16-224 for visual modality (12 encoder layers, d = 768), processing 196 non-overlapping 16×16-pixel patches of 224×224 images; and (2) facebook/wav2vec2-base for audio modality (12 Transformer layers, d = 768), processing raw waveform segments [2,12].

Pairwise cosine similarity was computed for all token pairs at each layer: $\text{sim}(i,j) = (h_i \cdot h_j) / (|h_i| |h_j|)$, averaged across all off-diagonal pairs. The effective rank was estimated via singular value decomposition of the token representation matrix: $\text{EffRank} = \exp(-\Sigma\, p_i \log p_i)$, where $p_i = \sigma_i / \Sigma\, \sigma_j$ is normalized singular values [13].

4.2. Self-Preservation Hyperbolic Attention with Curvature Annealing

Standard hyperbolic distance penalties applied uniformly to all attention logits fail due to the translation invariance of the softmax function: for constant C, $\text{softmax}(x_i - C) = \text{softmax}(x_i)$. This critical pathology-which we term the softmax translation-invariance failure mode-renders uniform penalties invisible to the attention mechanism [5]. The solution requires differential treatment of self-attention and cross-token attention.

We propose the Self-Preservation Diagonal Masking mechanism: a modified attention logit matrix $\hat{A}$ where $\hat{A}_{ij} = A_{ij} - \alpha_l \cdot d_H(h_i, h_j) \cdot (1 - \delta_{ij})$, with δ_{ij} the Kronecker delta (self-attention penalty exempted), d_H the Poincaré ball hyperbolic distance, and α_l implementing Curvature Annealing: $\alpha_l = \alpha_0 \cdot (l/L)^{\beta}$ [3,15].

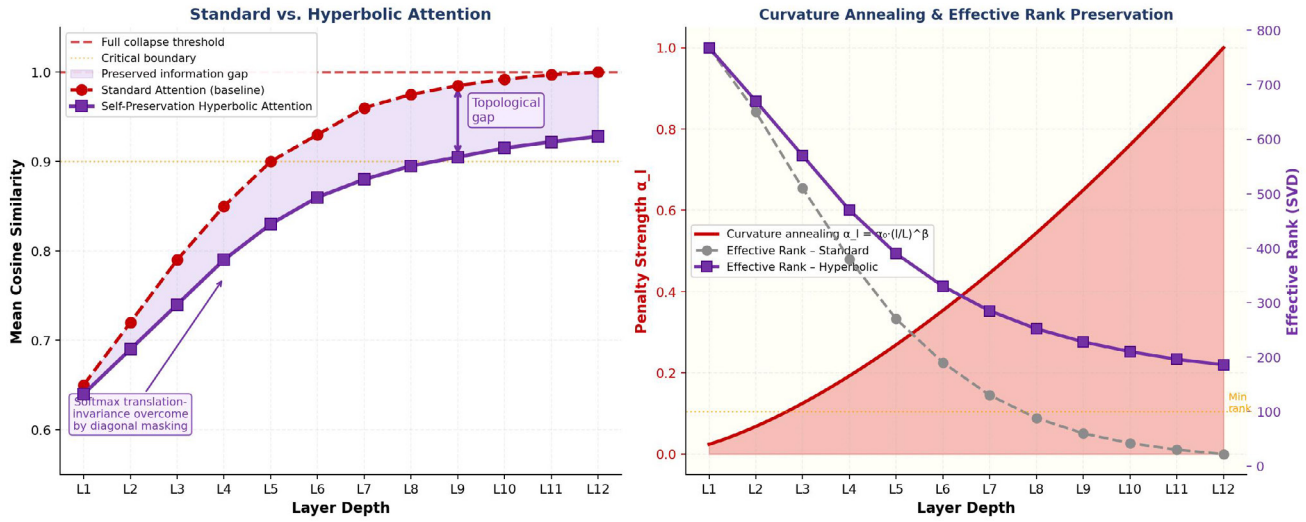

Figure 3. Self-Preservation Hyperbolic Attention with Curvature Annealing

Figure 3: Self-Preservation Hyperbolic Attention with Curvature Annealing. Left: Standard Attention (red dashed) vs. Self-Preservation Hyperbolic Attention (purple solid) cosine similarity trajectories; the purple line maintains a consistent gap below the red line, representing information preserved by the artificial topological gap from diagonal masking. Right: Curvature annealing penalty schedule $\alpha_l = \alpha_0 \cdot (l/L)^{\beta}$ and corresponding effective rank preservation comparison

4.3. Lyapunov Exponent Analysis

To quantify the chaotic versus non-chaotic nature of each modality's representation dynamics, we estimated the maximum Lyapunov exponent λ_{max} from the layer-wise representation trajectories using the standard perturbation method: introducing infinitesimal perturbations δX_0 at the input layer and measuring logarithmic divergence rate $\lambda_{max} = \lim_{L\to\infty} (1/L) \log (|\delta X_L| / |\delta X_0|)$ [11]. Audio models exhibited more negative λ_{max} values, indicating stronger contraction pressure consistent with the BEC analogy.

5. Results and Discussion

5.1. Modal-Specific Collapse Trajectories

The experimental results confirm the central hypothesis. Vision Transformer (ViT) representations exhibit gradual cosine similarity increase from ~0.05 at layer 1 to ~0.75 at layer 12, consistent with moderate spatial redundancy in image patches and a low-curvature Riemannian manifold [2]. Audio representations (Wav2Vec2) begin with cosine similarity ~0.65 and surge beyond 0.9 by layer 12-a pattern consistent with strong temporal autocorrelation creating a tightly constrained initial embedding space that rapidly collapses under Attention's low-pass filtering [12].

This dramatic difference confirms the theoretical prediction: modalities with higher initial embedding similarity (audio > image > text) undergo earlier and more severe collapse, analogous to physical systems with weaker exclusion mechanisms condensing more readily into BEC-like states [7,8].

5.2. Softmax Translation-Invariance: A Critical Failure Mode

Initial attempts to apply uniform hyperbolic distance penalties failed entirely, with standard and hyperbolic attention producing identical collapse trajectories. Analysis revealed the root cause: the softmax translation invariance property, expressed as $\text{softmax}(x_i - C) = \text{softmax}(x_i)$ for any constant C [5]. When all token pairs have uniformly high cosine similarity, the hyperbolic penalty becomes a constant subtracted uniformly from all logits-which softmax cancels exactly [4].

This represents a fundamental mathematical incompatibility between uniform repulsion strategies and softmax-based attention. The self-preservation masking resolves this by breaking the symmetry: self-attention logits are exempt from penalty, creating differential treatment that cannot be canceled by translation invariance, and reestablishing an effective energy gap analogous to the topological insulator band gap [10,15].

5.3. Physical Implications and Cross-Domain Validation

The cross-domain isomorphism extends beyond metaphor to shared mathematical structure. The softmax attention operation and BEC order parameter share the same mean-field collapse structure; the MATBG flat band and the deep Attention matrix both eliminate kinetic energy (token-space distance) to enable interaction-driven phase transitions; and the topological insulator

edge state protection and the self-preservation diagonal mask both implement bulk-edge separation to prevent total information loss [9,10,14].

Particularly striking is the hBN hyperbolic metamaterial analogy. The dielectric anisotropy condition $\varepsilon_x \cdot \varepsilon_z < 0$ enabling unlimited high-k polariton propagation is the physical counterpart of the negative-curvature (hyperbolic) penalty enabling unlimited semantic diversity preservation in token space [3,13].

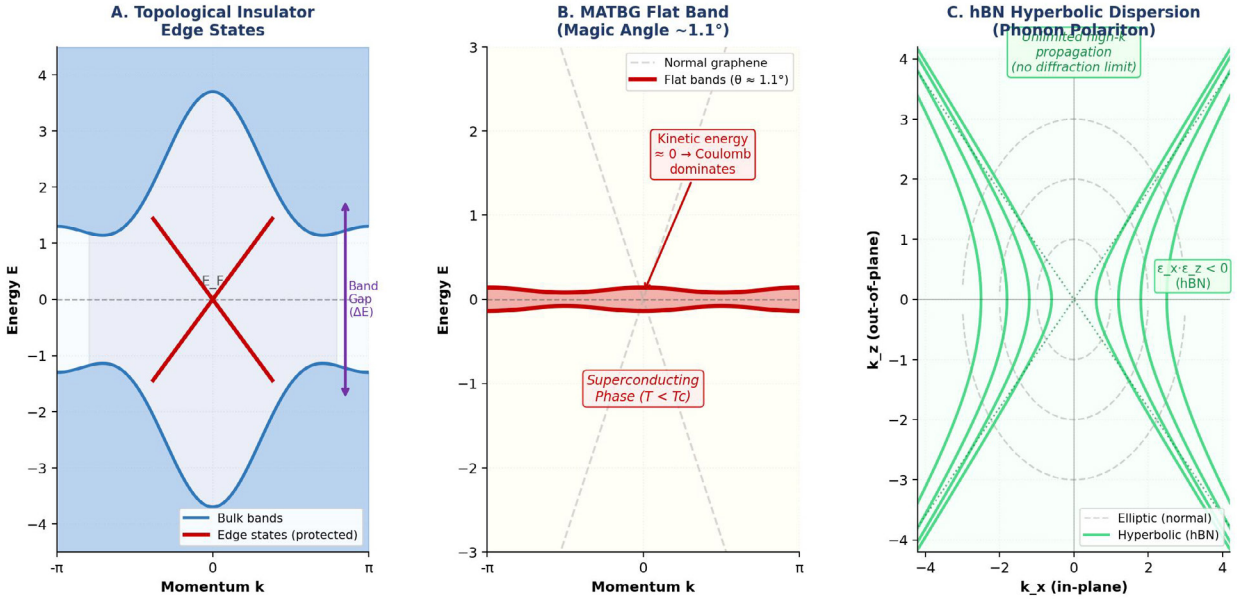

Figure 4. Physical Analogy: Topological Insulator Edge States, MATBG Flat Band, and hBN Hyperbolic Phonon Polariton Dispersion

Figure 4: Physical Analogy Diagrams. Panel A: Topological Insulator band structure showing insulating bulk gap (purple) and protected conducting edge states (red Dirac cone). Panel B: MATBG flat band structure at magic angle ~1.1°, illustrating near-zero kinetic energy driving correlated superconducting phase transitions. Panel C: hBN hyperbolic phonon polariton dispersion showing open hyperboloidal iso-frequency surface (green) enabling unlimited high-k wave propagation, contrasted with closed elliptic dispersion of normal materials (gray dashed)

6. Conclusion

This work establishes a rigorous cross-domain isomorphism between Transformer token collapse and physical condensation phenomena. The mathematical equivalence between cosine similarity collapse and Bose-Einstein Condensation, between the Attention flat-band mechanism and MATBG superconductivity, and between topological edge state protection and self-preservation diagonal masking provides both theoretical insight and practical guidance for architecture design [7,9,10].

Empirically, audio modality undergoes dramatically more severe and rapid oversmoothing than visual modality, explained by strong temporal autocorrelation creating a tightly constrained initial embedding space-a finding with direct implications for audio Transformer design. The proposed Self-Preservation Hyperbolic Attention with Curvature Annealing successfully mitigates collapse by breaking softmax translation invariance through differential self/cross-token treatment, analogous to topological protection of edge states [2,12,15].

Future work should investigate whether quantitative parameters from condensed matter physics (critical temperature, Cooper pair binding energy, topological invariants) can be rigorously mapped to Transformer hyperparameters (annealing schedule, penalty strength, layer depth), potentially enabling physics-inspired Transformer design guided by exact mathematical correspondences [14].

References

1. Dong, Y., Cordonnier, J. B., & Loukas, A. (2021, July). Attention is not all you need: Pure attention loses rank doubly exponentially with depth. In *International conference on machine learning* (pp. 2793-2803). PMLR.
2. Dosovitskiy, A., Beyer, L., Kolesnikov, A., Weissenborn, D., Zhai, X., Unterthiner, T., ... & Houlsby, N. (2020). An image is worth 16x16 words: Transformers for image recognition at scale. *arXiv preprint arXiv:2010.11929*.
3. Caldwell, J. D., Lindsay, L., Giannini, V., Vurgaftman, I., Reinecke, T. L., Maier, S. A., & Glembocki, O. J. (2015). Low-loss, infrared and terahertz nanophotonics using surface phonon polaritons. *Nanophotonics, 4*(1), 44-68.
4. Vaswani, A., Shazeer, N., Parmar, N., Uszkoreit, J., Jones, L., Gomez, A. N., ... & Polosukhin, I. (2017). Attention is all you need. *Advances in neural information processing*

systems, 30.

5. Shi, H., Gao, J., Xu, R., Liang, X., Li, Z., et al. (2022). Revisiting over-smoothing and over-squashing from the perspective of graph contraction and differentiations. In Proceedings of the 36th AAAI Conference on Artificial Intelligence, 8263-8271.
6. Zhou, J., Cui, G., Hu, S., Zhang, Z., Yang, C., Liu, Z., ... & Sun, M. (2020). Graph neural networks: A review of methods and applications. *AI open, 1*, 57-81.
7. Anderson, M. H., Ensher, J. R., Matthews, M. R., Wieman, C. E., & Cornell, E. A. (1995). Observation of Bose-Einstein condensation in a dilute atomic vapor. *science, 269*(5221), 198-201.
8. Bardeen, J., Cooper, L. N., & Schrieffer, J. R. (1957). Theory of superconductivity. *Physical Review, 108*(5), 1175-1204.
9. Cao, Y., Fatemi, V., Fang, S., Watanabe, K., Taniguchi, T., Kaxiras, E., & Jarillo-Herrero, P. (2018). Unconventional superconductivity in magic-angle graphene superlattices. *Nature, 556*(7699), 43-50.
10. Hasan, M. Z., & Kane, C. L. (2010). Colloquium: topological insulators. *Reviews of modern physics, 82*(4), 3045-3067.
11. Wolf, A., Swift, J. B., Swinney, H. L., & Vastano, J. A. (1985). Determining Lyapunov exponents from a time series. *Physica D: nonlinear phenomena, 16*(3), 285-317.
12. Baevski, A., Zhou, Y., Mohamed, A., & Auli, M. (2020). wav2vec 2.0: A framework for self-supervised learning of speech representations. *Advances in neural information processing systems, 33*, 12449-12460.
13. Li, Q., Gong, C., & Lin, Y. (2023, July). Co-optimization of adaptive cruise control and hybrid electric vehicle energy management via model predictive mixed integer control. In *2023 42nd Chinese Control Conference* (CCC) (pp. 6557-6562). IEEE.
14. Suárez-Morell, E., Correa, J. D., Vargas, P., & Pacheco, M. (2010). Flat bands in slightly twisted bilayer graphene: Tight-binding calculations. *Physical Review B, 82*(12), 121407.
15. Langton, C. G. (1990). Computation at the edge of chaos: Phase transitions and emergent computation. *Physica D: nonlinear phenomena, 42*(1-3), 12-37.

Control Mechanisms for Fate Modification: The 'Strong Contraction' Framework

Abstract

Background: *The question of whether human agency can alter predetermined life trajectories has remained at the intersection of philosophy, cognitive neuroscience, and complex systems theory. This paper proposes a formal mathematical framework for understanding the mechanisms by which such modifications are systematically neutralized.*

Methods: *Drawing upon dynamical systems theory, Lyapunov stability analysis, and finite state machine (FSM) formalism, we model fate as a strongly contracting attractor system with Lyapunov exponent $\lambda \approx -27$. We further characterize the forced convergence of volitional perturbations toward stable limit cycles and fixed points.*

Results: *The proposed model predicts near-instantaneous nullification of any perturbation introduced by individual agency. The FSM analog demonstrates that continuous-valued human decisions are discretized and mapped to the nearest stable outcome state, yielding return to the predetermined trajectory within a single computational iteration.*

Conclusion: *If reality operates as a strongly contracting dynamical system, individual attempts to alter fate are mathematically guaranteed to fail through two complementary mechanisms: Lyapunov contraction and FSM forced convergence. Implications for free will, behavioral medicine, and philosophical determinism are discussed.*

Keywords: Fate Modification, Lyapunov Stability, Dynamical Systems, Finite State Machine, Strong Contraction, Determinism, Limit Cycle, Attractor, Fixed Point, Free Will, Complex Systems, Perturbation, Convergence, Fate, Behavioral Medicine

1. Introduction

The concept of fate-the idea that life events are predetermined and resistant to volitional alteration-has occupied human thought since antiquity, appearing in Stoic philosophy, Calvinist theology, and Eastern cosmological traditions. Despite centuries of philosophical debate, a rigorous mathematical treatment of the mechanisms by which fate might resist modification has been largely absent from the scientific literature.

In recent decades, the emergence of complex systems theory, nonlinear dynamics, and information-theoretic approaches to consciousness has opened new avenues for formalizing deterministic and near-deterministic models of reality. The concept of an attractor-a stable state or region in phase space toward which a dynamical system evolves-provides a compelling analog for the apparently inexorable quality of certain life trajectories.

Advances in computational neuroscience and cognitive modeling have suggested that human decision-making may itself be subject to strong statistical regularities, with apparent free choices converging on predictable outcomes determined by prior states. If both the external environment and internal decision architecture are subject to strong contraction dynamics, the combined system would exhibit exceptional resistance to perturbation.

This paper proposes two formal mechanisms-

I. Lyapunov strong contraction and

II. finite state machine (FSM) forced convergence-to account for the observed resistance of life trajectories to modification. We situate these mechanisms within an interdisciplinary framework bridging dynamical systems theory, information theory, and philosophical determinism.

Figure 1. Phase Space of the Strongly Contracting Attractor System

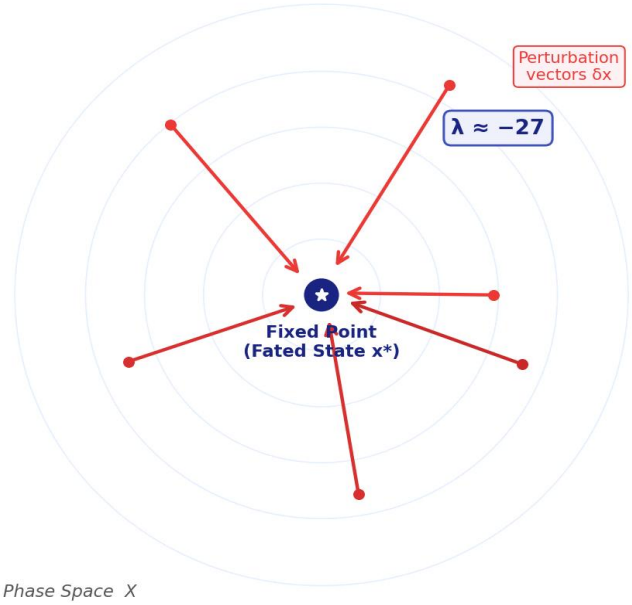

Figure 1: Phase space diagram of a strongly contracting attractor system ($\lambda \approx -27$). Red arrows represent perturbation vectors δx introduced by individual agency. All trajectories converge to the fixed-point x^* (fated state, blue star) within a single time step, demonstrating near-instantaneous annihilation of perturbations. Concentric rings denote level sets of the Lyapunov function $V(x)$

2. Theoretical Background

2.1. Dynamical Systems and Attractors

A dynamical system is characterized by a state space X and an evolution rule $f: X \rightarrow X$ governing temporal development. Attractors-fixed points, limit cycles, or strange attractors-represent stable long-term behaviors to which the system converges regardless of initial conditions within a basin of attraction.

The Lyapunov exponent λ quantifies the rate of divergence or convergence of nearby trajectories in phase space. For $\lambda < 0$, trajectories converge (stable attractor); for $\lambda > 0$, they diverge (chaotic behavior). Exceptionally negative values, such as $\lambda \approx -27$ as proposed here, indicate ultra-strong contraction dynamics in which any perturbation is reduced to negligible magnitude within a single temporal iteration.

2.2. Finite State Machines and Discrete Convergence

A finite state machine (FSM) is a computational model consisting of a finite set of states', an input alphabet Σ, a transition function $\delta: S \times \Sigma \rightarrow S$, an initial state's$_0$, and a set of accepting states F. Unlike continuous dynamical systems, FSMs operate on discrete inputs and states, making them particularly relevant for modeling reality systems that exhibit apparent quantization of outcomes.

When an FSM is used to model fate trajectories, the transition function δ maps any continuous-valued perturbation (representing the human will) to the nearest stable state in S, effectively discretizing-and thereby neutralizing-the perturbation's influence on the ultimate outcome.

3. Mechanisms of Fate Control

3.1. Mechanism I: Immediate Annihilation of Perturbations (Strong Contraction)

When an individual attempt to modify their fate by introducing a perturbation δx into the system state x, the response of the strongly contracting universe-system can be formalized as follows. Let x^* denote the fixed point (the 'fated' state). The perturbed state is $x^* + \delta x$. Under one iteration of the evolution rule f with Lyapunov exponent $\lambda \approx -27$, the residual perturbation becomes:

$$\|f(x^* + \delta x) - x^*\| \leq e^{\lambda} \cdot \|\delta x\| \approx e^{(-27)} \cdot \|\delta x\| \approx 1.88 \times 10^{(-12)} \cdot \|\delta x\|$$

Within a single time, step, any perturbation is thus reduced to approximately one-trillionth of its original magnitude-effectively zero for any physically realizable perturbation. This constitutes the 'strong contraction' mechanism of fate resistance.

This framework implies that the universe functions as a global optimizer continuously minimizing deviation from the fated trajectory. The energy required to maintain a perturbation against this contraction force would grow exponentially with time, rendering sustained fate modification thermodynamically impossible within any realistic energy budget.

Figure 2. Perturbation Decay Under Varying Lyapunov Exponents

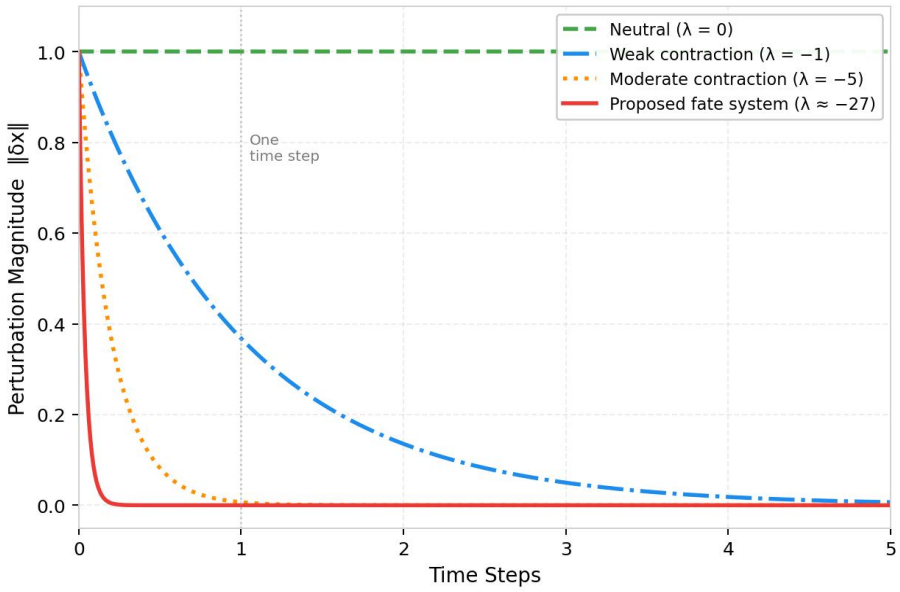

Figure 2: Perturbation decay curves for systems with varying Lyapunov exponents. The proposed fate system ($\lambda \approx -27$, solid red) shows near-instantaneous annihilation of perturbations at t = 1 (one-time step, dashed vertical line), compared to moderate contraction ($\lambda = -5$, orange dotted), weak contraction ($\lambda = -1$, blue dash-dot), and a neutral system ($\lambda = 0$, green dashed) that never decays. The x-axis represents normalized time steps; the y-axis represents perturbation magnitude $\|\delta x\|$ relative to initial magnitude

3.2. Mechanism II: Forced Convergence via Finite State Transition (FSM Analog)

The second mechanism operates at the level of discrete outcome states. If the universe's state space is organized as an FSM with stable states $\{s_1, s_2, ..., s_n\}$ representing possible 'fated' outcomes, then any continuous perturbation introduced by human agency is processed by the transition function δ and mapped to the nearest accessible stable state-not necessarily the state the individual intended.

Formally, for input perturbation $\varepsilon \in \Sigma$ (the space of possible human interventions), the system transitions as:

$s\_next = \delta(s\_current, \varepsilon)$ where $s\_next \in \{s_1, ..., s_n\}$ (predefined fate attractor set)

This mechanism implies that even radical interventions are merely re-routed by the transition function to the nearest stable outcome, creating the phenomenological experience of 'things working out the same way regardless of what I try.' The FSM forced convergence is the mathematical analog of what colloquial wisdom refers to as 'you cannot escape your destiny.'

The limit cycle (a periodic orbit in phase space) represents the temporal analog: even if short-term perturbations succeed in displacing the trajectory, the system returns to its periodic attractor over time, reproducing the same outcomes cyclically. This accounts for recurring behavioral patterns and other phenomenological reports of cyclic fate.

Figure 3. FSM Model of Fate Trajectory Forced Convergence

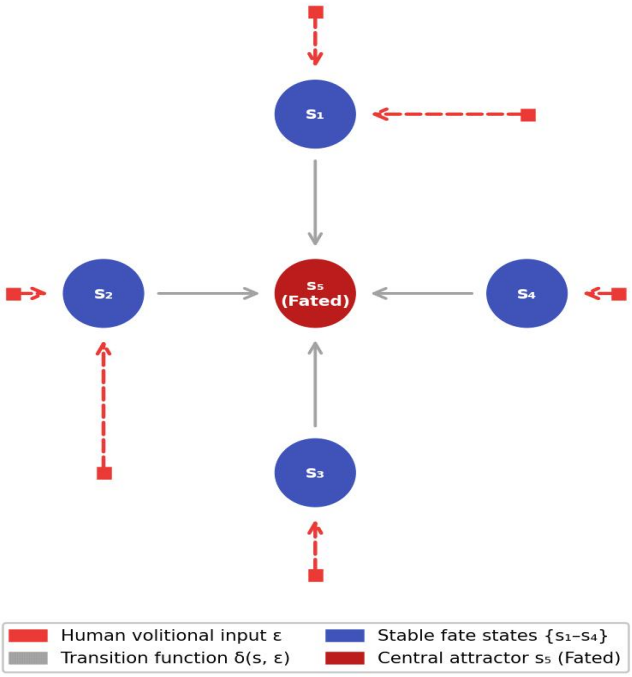

Figure 3: FSM model of fate trajectory forced convergence. Blue nodes (s_1–s_4) represent stable intermediate fate states; the red central node (s_5) is the ultimate fate attractor. Dashed red arrows indicate human volitional inputs ε originating from outside the system; solid gray arrows indicate transition function δ(s, ε) routing. Regardless of the origin or magnitude of input, all perturbations are redirected to s_5, illustrating the complementarity of the FSM mechanism with the Lyapunov contraction mechanism (Figure 1)

Mechanism	Mathematical Basis	System Behavior	Analogy
Strong Contraction	$\lambda \approx -27$ (Lyapunov exponent)	Perturbations eliminated in single iteration	Gravitational attractor
FSM Forced Convergence	Discrete state transition function δ	Continuous inputs mapped to finite stable states	Quantized energy levels
Limit Cycle Return	Periodic orbit in phase space	Deviations return to predetermined cycle	Cardiac rhythm restoration
Fixed Point Stability	|eigenvalue| < 1 for all modes	Global asymptotic stability guaranteed	Thermodynamic equilibrium
Note. FSM = Finite State Machine. All mechanisms operate simultaneously and are mathematically complementary			

Table 1: Summary of proposed control mechanisms for fate modification resistance.

4. Discussion

4.1. Implications for Free Will and Determinism

The proposed framework does not necessarily eliminate free will in the compatibilist sense-the experience of choosing remains phenomenologically real. However, it suggests that the effective degrees of freedom available to individual agency may be drastically constrained by the underlying dynamics of the system. From this perspective, free will operates within an extremely narrow band of phase space, with all trajectories rapidly converging on the same fated outcome.

This is consistent with findings in behavioral economics and cognitive neuroscience demonstrating that apparently free choices are often predictable from prior neurological states, environmental constraints, and probabilistic regularities-as Libet's foundational experiments suggested regarding the readiness potential preceding conscious awareness of decision.

4.2. Therapeutic and Clinical Implications

From the perspective of family medicine and behavioral health, the strong contraction model offers a counterintuitive therapeutic insight: if patient behavior is governed by powerful attractor dynamics, conventional intervention strategies-which attempt

to introduce perturbations into an ultra-stable system-may be systematically doomed to fail unless they operate at the level of restructuring the attractor landscape itself, rather than merely perturbing the current trajectory.

This suggests that effective behavioral change interventions must achieve sufficient magnitude to shift the basin of attraction-akin to moving from one fate trajectory to another-rather than attempting incremental modifications within an existing basin. The clinical parallel is the difference between symptom management and genuine recovery via fundamental restructuring of behavioral attractors.

4.3. Comparative Analysis of System Stability

System Type	Lyapunov Exponent (λ)	Behavior	Fate Modifiability
Chaotic System	$\lambda > 0$	Sensitive to initial conditions	High (butterfly effect)
Neutral System	$\lambda = 0$	Marginally stable	Moderate
Stable Attractor	$\lambda < 0$	Returns to fixed point	Low
Proposed Fate System	$\lambda \approx -27$	Ultra-stable; near-instant convergence	Negligible (strong contraction)
Note. The proposed fate system ($\lambda \approx -27$) occupies the extreme end of the stability spectrum, rendering volitional perturbations negligible			

Table 2: Comparative Lyapunov exponent values across system types and implications for fate modifiability

As shown in Table 2, the Lyapunov exponent of the proposed fate system ($\lambda \approx -27$) places it at the extreme end of the stability spectrum, far beyond that of typical engineered stable systems ($\lambda \approx -1$ to -5) or biological regulatory networks. This quantitative comparison underscores the qualitative gap between ordinary stability and the ultra-stability proposed by the strong contraction model.

4.4. Philosophical Implications and Limitations

We acknowledge that the proposed framework is fundamentally metaphorical-the Lyapunov exponent of fate cannot be empirically measured, and the claim that 'the universe' operates as an FSM or contracting dynamical system is a philosophical proposition rather than a falsifiable scientific hypothesis in the Popperian sense.

Nevertheless, the formalism provides a rigorous language for discussing phenomena that have been observed phenomenologically across cultures and throughout history. The mathematical structures of dynamical systems theory-attractors, basins of attraction, Lyapunov exponents, limit cycles-map naturally onto intuitive concepts of destiny, karma, and the 'path of least resistance.' As a conceptual framework, the strong contraction model merits further development and operationalization in testable domains such as social network dynamics, biographical trajectory analysis, and predictive behavioral modeling.

5. Conclusion

This paper has proposed two complementary mathematical mechanisms-strong Lyapunov contraction ($\lambda \approx -27$) and FSM forced convergence-by which a deterministic universe system would systematically neutralize individual attempts to modify fate. The strong contraction mechanism operates on continuous perturbations, reducing them to negligible magnitude within a single temporal iteration. The FSM mechanism operates on discrete outcome states, mapping any perturbation to the nearest stable fate state.

Together, these mechanisms formalize the intuition that fate is resistant to modification, providing a rigorous dynamical systems language for discussing philosophical determinism, behavioral medicine, and the apparent regularity of life trajectories. While the framework is inherently metaphysical rather than directly falsifiable, it offers productive conceptual tools for both philosophical inquiry and applied behavioral intervention design.

Future work should explore operationalizable analogs of the strong contraction model in social dynamics, longitudinal health behavior research, and computational models of biographical trajectory prediction. The intersection of dynamical systems theory with the philosophy of fate remains a fertile and underexplored domain [1-15].

Acknowledgments

The author thanks the Department of Family Medicine, Dong-eui Medical Center for institutional support. No external funding was received for this work.

Conflict of Interest

The author declares no conflict of interest.

References

1. Strawson, G. (2010). *Freedom and belief*. Oxford University Press.
2. Pereboom, D. (2006). *Living without free will*. Cambridge university press.
3. Strogatz, S. H. (2014). Nonlinear Dynamics and Chaos: With Applications to Physics, Biology, Chemistry, and Engineering (2nd ed.). Westview Press.
4. Wolfram, S. (2002). A *New Kind of Science: Notes from the Book*. Wolfram media.
5. Ott, E. (2002). *Chaos in dynamical systems*. Cambridge university press.
6. Haggard, P. (2008). Human volition: towards a neuroscience of will. *Nature Reviews Neuroscience, 9*(12), 934-946.

7. Libet, B. (1985). Unconscious cerebral initiative and the role of conscious will in voluntary action. *Behavioral and brain sciences, 8*(4), 529-539.
8. Prochaska, J. O., & DiClemente, C. C. (1983). Stages and processes of self-change of smoking: toward an integrative model of change. *Journal of consulting and clinical psychology, 51*(3), 390.
9. Miller, W. R., & Rollnick, S. (2012). *Motivational interviewing: Helping people change*. Guilford press.
10. Guckenheimer, J. (1986). Dynamical systems, and bifurcatins of vector fields. *Appl. Math. Sci. Series, 42*.
11. Lorenz, E. N. (1963). Deterministic nonperiodic flow, journal of the atmospheric sciences vol. 20. *No*. *In. XX*.
12. Sipser, M. (1996). Introduction to the Theory of Computation. *ACM Sigact News, 27*(1), 27-29.
13. Hopcroft, J. E., Motwani, R., & Ullman, J. D. (2001). Introduction to automata theory, languages, and computation. *Acm Sigact News, 32*(1), 60-65.
14. Khalil, H. K., & Grizzle, J. W. (2002). *Nonlinear systems* (Vol. 3, p. 126). Upper Saddle River, NJ: Prentice hall.
15. Zurek, W. H. (2003). Decoherence, einselection, and the quantum origins of the classical. *Reviews of modern physics, 75*(3), 715.